

Rubidium-87 NMR Study of Ion Interaction with the Gramicidin Transmembrane Channel

D. W. Urry,* T. L. Trapane, C. M. Venkatachalam, and K. U. Prasad

Contribution from the Laboratory of Molecular Biophysics, School of Medicine, University of Alabama at Birmingham, P.O. Box 311/University Station, Birmingham, Alabama 35294.
Received July 26, 1985

Abstract: Rubidium-87 NMR studies are reported on the interaction of rubidium ion with the gramicidin transmembrane channel. Useful changes in the magnitude of the longitudinal relaxation times and large negative chemical shifts are observed on interaction with the channel. These changes were utilized to estimate the magnitude of two binding constants, a tight binding constant, K_b^* > 30 M⁻¹, and a weak binding constant, K_b^w , in the range of 1 to 4 M⁻¹. Additionally at 0.55 M RbCl concentration the resonance line shape was clearly non-Lorentzian with the resolution of two components having transverse relaxation times of $T_2' \approx 0.058$ ms and $T_2'' \approx 0.37$ ms. At an ion activity of 1.5 M RbCl with use of a null approach, $T_2' = 0.151$ ms and $T_2'' = 0.753$ ms. Both sets of values were used in the Bull analysis to give the same ion correlation time which was then used to estimate the off-rate constant from the doubly occupied state of the channel, i.e., $k_{off}^{**} \approx 7.7 \times 10^7$ s⁻¹. The rubidium-87 NMR derived binding constant for double ion occupancy and off-rate constant for the doubly occupied state were used to calculate a net current through the channel by means of Eyring rate theory, the known channel structure, and the binding site locations to introduce voltage dependence. The calculated current, using the rubidium-87 NMR derived binding and rate constants, gave values in close agreement with those obtained from electrical measurements of single channel rubidium ion currents. Also the same binding and rate constants were compared for rubidium-87 and sodium-23 to obtain an estimate of the conductance ratios for these ions which again compared favorably with the ion transport studies. Thus rubidium-87 NMR, for which previously there has been demonstrated only limited utility, is shown here with a standard high-resolution spectrometer to be useful for characterizing ion interactions relevant to ion transport, and the Bull analysis for spin 3/2 nuclei is seen to give relative values for correlation times that correspond to relative conductances.

The gramicidin transmembrane channel provides a particularly appealing molecular system on which to utilize nuclear magnetic resonance methods for characterizing the interactions of ions having quadrupolar nuclei. This is because (1) the magnitudes of the currents of ions passing through the channel are in the range of 10⁷ to 10⁸ ion/s,¹⁻⁶ giving favorable rates in relation to the available observation frequencies, (2) the relative conductances of the alkali metal ions (Li⁺, Na⁺, K⁺, Rb⁺, and Cs⁺) are well-known,⁶⁻⁹ (3) the channel structure has a twofold symmetry axis perpendicular to the channel axis,¹⁰⁻¹³ (4) the channel structure¹¹ requires single filing of ions and water,¹⁴⁻¹⁹ (5) the ion translocation rate from one side of the channel to the other (i.e.,

from one binding site at one mouth of the channel to the other) is not rate limiting,²⁰⁻²² and (6) the rate of ion entry and leaving is only weakly voltage dependent.²³ Thus a comparison, among the group IA (group 1) elements, of quadrupolar ion nuclear magnetic resonance studies provides an opportunity to evaluate the efficacy of transverse relaxation time (T_2) analyses such as those of Bull, Forsén, and colleagues^{24,25} relative to estimates of correlation times and the translation of those into rate constants and to evaluate the effectiveness of using longitudinal relaxation time (T_1) analyses²⁴⁻²⁶ and chemical shifts in estimating binding constants. Previous quadrupolar ion interaction studies on the gramicidin transmembrane channel have been reported on lithium ion,²⁷ sodium ion,²⁸⁻³⁰ potassium ion,³¹ and cesium ion.³²

The present paper treats the rubidium ion interactions with the gramicidin transmembrane channel with use of primarily rubidium-87 NMR. Previous studies using rubidium NMR are few, some directed toward solids³³ and nonaqueous solvents³⁴ and a few related to the interactions with synthetic organic molecules³⁵ and biomolecules.^{36,37} To our knowledge this report represents

- (1) Lauger, P. *Biochim. Biophys. Acta* **1973**, *311*, 423-441.
- (2) Bamberg, E.; Kolb, H. A.; Lauger, P. In *The Structural Basis of Membrane Function*; Academic Press, Inc.: New York, 1976; pp 143-157.
- (3) Sandblom, J.; Eisenman, G.; Hagglund, J. *J. Membr. Biol.* **1983**, *71*, 61-78.
- (4) Urry, D. W. In *Topics in Current Chemistry*; Boschke, F. L., Ed.; Springer-Verlag: Heidelberg, Germany, 1985; Vol. 128, pp 175-218.
- (5) Finkelstein, A.; Andersen, O. S. *J. Membrane Biol.* **1981**, *59*, 155-171.
- (6) Hladky, S. B.; Haydon, D. A. *Curr. Top. Membr. Transp.* **1984**, *21*, 327-372.
- (7) Hladky, S. B.; Haydon, D. A. *Biochim. Biophys. Acta* **1972**, *274*, 294-312.
- (8) Bamberg, E.; Noda, K.; Gross, E.; Lauger, P. *Biochim. Biophys. Acta* **1976**, *419*, 223-228.
- (9) Eisenman, G.; Sandblom, J.; Neher, E. *Biophys. J.* **1978**, *22*, 307-340.
- (10) Urry, D. W.; Goodall, M. C.; Glickson, J. D.; Mayers, D. F. *Proc. Natl. Acad. Sci. U.S.A.* **1971**, *68*, 1907-1911.
- (11) Urry, D. W. In *The Enzymes of Biological Membranes*; Martonosi, A. N., Ed.; Plenum Publishing Corp.: New York, 1985; pp 229-257.
- (12) Urry, D. W.; Trapane, T. L.; Prasad, K. U. *Science* **1983**, *221*, 1064-1067.
- (13) Weinstein, S.; Wallace, B. A.; Blout, E. R.; Morrow, J. S.; Veatch, W. *Proc. Natl. Acad. Sci. U.S.A.* **1979**, *76*, 4230-4234.
- (14) Rosenberg, P. A.; Finkelstein, A. *J. Gen. Physiol.* **1978**, *72*, 327-340.
- (15) Rosenberg, P. A.; Finkelstein, A. *J. Gen. Physiol.* **1978**, *72*, 341-350.
- (16) Dani, J. A.; Levitt, D. G. *Biophys. J.* **1981**, *35*, 485-499.
- (17) Dani, J. A.; Levitt, D. G. *Biophys. J.* **1981**, *35*, 501-508.
- (18) Kim, K. S.; Vercouteren, D. P.; Welti, M.; Chin, S.; Clementi, E. *Biophys. J.* **1985**, *47*, 327-335.
- (19) Mackay, D. H. J.; Berens, P. H.; Wilson, K. R.; Haglar, A. T. *Biophys. J.* **1984**, *46*, 229-248.

- (20) Andersen, O. S. *Biophys. J.* **1983**, *41*, 119-133.
- (21) Hladky, S. B. *Biophys. J.* **1985**, *47*, 747.
- (22) Andersen, O. S. *Biophys. J.* **1985**, *47*, 747-749.
- (23) Eisenman, G.; Sandblom, J.; Hagglund, J. In *Structure and Function of Excitable Cells*; Chang, D. C., Tasaki, I., Adelman, W. J., Leuchtag, H., Eds.; Plenum Publishing Corp.: New York, 1983; pp 383-413.
- (24) Bull, T. E. *J. Magn. Reson.* **1972**, *8*, 344-353.
- (25) Bull, T. E.; Forsén, S.; Turner, D. L. *J. Chem. Phys.* **1979**, *70*, 3106-3111.
- (26) James, T. L.; Noggle, J. H. *Proc. Natl. Acad. Sci. U.S.A.* **1969**, *62*, 644-649.
- (27) Urry, D. W.; Trapane, T. L.; Venkatachalam, C. M.; Prasad, K. U. *J. Phys. Chem.* **1983**, *87*, 2918-2923.
- (28) Urry, D. W.; Venkatachalam, C. M.; Spisni, A.; Lauger, P.; Khaled, M. A.; *Proc. Natl. Acad. Sci. U.S.A.* **1980**, *77*, 2028-2032.
- (29) Venkatachalam, C. M.; Urry, D. W. *J. Magn. Reson.* **1980**, *41*, 313-335.
- (30) Urry, D. W.; Venkatachalam, C. M.; Spisni, A.; Bradley, R. J.; Trapane, T. L.; Prasad, K. U. *J. Membr. Biol.* **1980**, *55*, 29-51.
- (31) Urry, D. W.; Trapane, T. L.; Venkatachalam, C. M.; Prasad, K. U. *Can. J. Chem.* **1985**, *63*, 1976-1981.
- (32) Urry, D. W.; Trapane, T. L.; Brown, R. A.; Venkatachalam, C. M.; Prasad, K. U. *J. Magn. Reson.* **1985**, *65*, 43-61.
- (33) Segel, S. L. *J. Chem. Phys.* **1980**, *73*, 4146-4147.
- (34) Popov, A. I. *Pure Appl. Chem.* **1979**, *51*, 101-110.
- (35) Khazaeli, S.; Dye, J. L.; Popov, A. I. *Spectrochim. Acta* **1983**, *39A*, 19-21.
- (36) Lindman, B.; Lindqvist, I. *Chem. Scr.* **1971**, *1*, 195-196.

the first use of rubidium-87 NMR to estimate binding and rate constants relative to ion interaction with biological molecules in aqueous systems. Interestingly it does so on an ion transport system which is the first characterized ion selective transmembrane channel, one that serves as a model for transport in higher organisms. Furthermore, this molecular system allows comparisons of the efficacy of the several quadrupolar ion NMR approaches to interactions of the alkali metal ions.

The primary structure of gramicidin A (GA) is HCO-L-Val¹-Gly²-L-Ala³-D-Leu⁴-L-Ala⁵-D-Val⁶-L-Val⁷-D-Val⁸-L-Trp⁹-D-Leu¹⁰-L-Trp¹¹-D-Leu¹²-L-Trp¹³-D-Leu¹⁴-L-Trp¹⁵-NHCH₂CH₂OH.³⁸ When in the channel state, GA forms a single-stranded, left-handed, β -helical conformation^{10,39} in which there are 6.2 to 6.3 residues per turn of helix.⁴⁰ Two β -helical molecules associate head to head (formyl end to formyl end) by means of six intermolecular hydrogen bonds to form a lipid membrane spanning structure about 26 Å long (as a repeat distance) and with a 4 Å (maximal) diameter channel coincident with the helix axis as proposed in 1971.¹⁰ With use of carbon-13 NMR to monitor ion induced carbonyl carbon chemical shifts exhibited by the channel state which is formed by singly carbonyl carbon enriched GA molecules, two symmetry related binding sites have been observed.⁴¹ The distance separating the two sites is an angstrom or two less for Tl⁺ than for Na⁺, and the accuracy of the distance depends on the accuracy (within the lipid membrane) of the value of h , the translation distance along the helix for the repeating dipeptide unit, and on the length of the hydrogen bonds at the head-to-head junction. A value of 22–23 Å seems most reasonable for the distance separating the two ion binding sites with the ion position along the channel axis being between the positions of the carbonyl oxygens of the Trp¹³ and Trp¹¹ residues.

It has been demonstrated that the channel state can be obtained in lipid bilayers by heat incubation of gramicidin with L- α -lysophosphatidylcholine, also referred to as lysophosphatidylcholine or lyso-PC. In this system it can be demonstrated with the singly carbonyl carbon enriched gramicidin A, e.g., (1-¹³C)Trp¹³-GA, that more than 90% of the molecules, i.e., specifically in this example more than 90% of the Trp¹³ carbonyls, are accessible for ion interaction.³² Another advantage of this incorporation of the channel state into phospholipid bilayers^{43,44} is that with lyso-PC there is relatively poor sealing of bilayer vesicles such that this limits the problems of having separate extravascular and intravesicular compartments.³² The view is that with lyso-PC the bilayer state is just as readily described as bilayer sheets. Accordingly this is the system that has been used in our previous and the present quadrupolar ion NMR studies.

The present effort reports rubidium-87 chemical shifts, longitudinal relaxation times (T_1), and line shape data as a function of concentration of RbCl in ²H₂O, in lyso-PC in ²H₂O, and in the channel-lyso-PC system in ²H₂O with 3 mM channels. Both broad and narrow components are observed in the resonances of this spin ³/₂ system only in the presence of channels. Estimates are made for binding constants for the tight (single ion occupancy) and weak (double ion occupancy) sites with use of chemical shift and T_1 data. In the latter case both standard T_1 analyses are used as well as separate determinations of T_1' and T_1'' for the narrow and broad components, respectively, by estimating the inversion times (null points) separately for each component. From the line shape at high ion concentrations the line widths of both the broad and narrow components are used to estimate T_2' and T_2'' , and by using

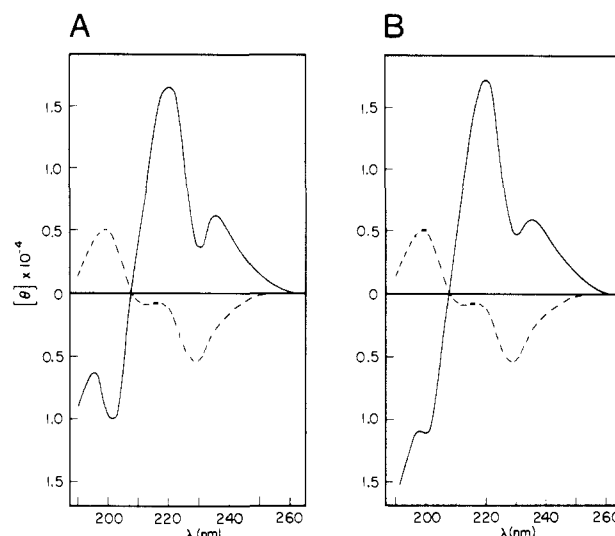


Figure 1. Circular dichroism spectra in H₂O of lysolecithin packaged (1-¹³C)Trp¹³ gramicidin A (A) and natural gramicidin (B). Both spectra show complete incorporation of the peptide channel into the lipid. This should be verified before ion interaction studies are begun. When gramicidin has associated with the lipid but has not yet begun conversion to the proper channel state, a spectrum such as the one indicated by the dashed curve is obtained.

the Bull analysis²⁴ the ion correlation time, τ_c , is calculated. Recognizing that the bilayer structure containing the channels and hence the channels themselves have long reorientation correlation times and presenting arguments that indicate vibration of the electric field gradients is not the dominant relaxation mechanism, the inverse of τ_c is taken as an estimate for the off-rate constant for an ion leaving the doubly occupied channel, k_{off}^w . The single channel current for rubidium ion, with the known structure of the channel and an estimate of the weak voltage dependence of the off-rate constant, can be calculated from the NMR-derived weak binding constant, K_b^w , and the off-rate constant from the weak site. The single channel current calculated with use of the NMR-derived binding and rate constants compares favorably with the experimental determination of currents, that is, this comparison for the rubidium ion is found to be favorable as it has been for the sodium ion.^{28,30} Furthermore the ratio of $k_{off}^w(\text{Rb}^+)/k_{off}^w(\text{Na}^+)$ derived from the Bull analysis²⁴ is close to the conductance ratio, $\gamma(\text{Rb}^+)/\gamma(\text{Na}^+)$, derived from the channel conductance studies.

Materials and Methods

Commercially available gramicidin (ICN Nutritional Biochemicals, Cleveland, OH) which is 72% GA, 19% Tyr¹¹-GA(GC), and 9% Phe¹¹-GA(GB) was lyophilized from methanol-water suspension and used without further purification in the rubidium-87 studies. L- α -Lysophosphatidylcholine (lyso-PC) was purchased as a lyophilized powder from Avanti Polar Lipids, Inc., Birmingham, AL, and was verified to be pure by carbon-13 NMR. Deuterium oxide (²H₂O, 99.87% ²H) purchased from Sci-Graphics, Wayne, NJ, and rubidium chloride obtained from Aldrich Chemical Co., Inc., Milwaukee, WI (Gold Label Lot No. 0397), were used as received.

(1-¹³C)Trp¹³-gramicidin A was synthesized by the solid-phase methodology⁴⁵ as described earlier.^{46,47} Briefly, starting from *tert*-butyloxycarbonyl (Boc)Trp-Resin, each subsequent amino acid was added following essentially (1) the decoupling step with 33% TFA/CH₂Cl₂ containing 5% 1,2-ethanedithiol and 6% anisole, (2) the neutralization step with 5% diisopropylethylamine/CH₂Cl₂, and (3) the coupling step with 2.5 equiv of Boc-amino acid and dicyclohexylcarbodiimide. After the synthesis was completed, the peptide was removed from the resin by ethanolamine treatment, the N^α-Boc-group was removed, and the peptide was formylated. The peptide was purified by ion-exchange chromatography, preparative thin-layer chromatography (TLC), followed by LH-20 column chromatography. The purity of the peptide was established by

(45) Merrifield, R. B. *J. Am. Chem. Soc.* **1963**, *85*, 2149–2154.

(46) Prasad, K. U.; Trapane, T. L.; Busath, D.; Szabo, G.; Urry, D. W. *Int. J. Pept. Protein Res.* **1982**, *19*, 162–171.

(47) Prasad, K. U.; Trapane, T. L.; Busath, D.; Szabo, G.; Urry, D. W. *Int. J. Pept. Protein Res.* **1983**, 341–347.

(37) Detellier, C.; Lazlo, P. *J. Am. Chem. Soc.* **1980**, *102*, 1135–1141.

(38) Sarges, R.; Witkop, B. *J. Am. Chem. Soc.* **1965**, *87*, 2011–2020.

(39) Urry, D. W.; Long, M. M.; Jacobs, M.; Harris, R. D. *Ann. N.Y. Acad. Sci.* **1975**, *264*, 203–220.

(40) Venkatachalam, C. M.; Urry, D. W. *J. Comput. Chem.* **1983**, *4*, 461–469.

(41) Urry, D. W.; Prasad, K. U.; Trapane, T. L. *Proc. Natl. Acad. Sci. U.S.A.* **1982**, *79*, 390–394.

(42) Urry, D. W.; Spisni, A.; Khaled, M. A. *Biochem. Biophys. Res. Commun.* **1979**, *88*, 940–949.

(43) Spisni, A.; Pasquali-Ronchetti, I.; Casali, E.; Lindner, L.; Cavatorta, L.; Masotti, L.; Urry, D. W. *Biochim. Biophys. Acta* **1983**, *732*, 58–68.

(44) Killian, J. A.; De Kruijff, B.; Van Echteld, C. J. A.; Verkleij, A. J.; Leunissen-Bijvelt, J.; De Gier, J. *Biochim. Biophys. Acta* **1983**, *728*, 141–144.

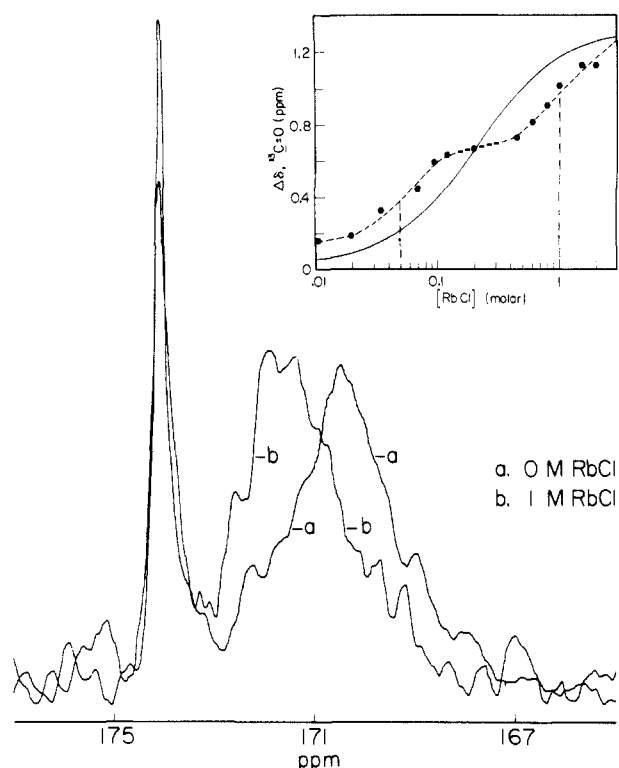


Figure 2. Carbon-13 nuclear magnetic resonance spectra at 70 °C of lysolecithin packaged ($1\text{-}^{13}\text{C}$)-enriched Trp^{13} gramicidin A. Curve a is without and curve b is with 1 M rubidium ion present; the comparison shows the change in the chemical shift of the labeled carbonyl upon addition of RbCl . The inset gives the dependence on RbCl concentration of this carbonyl carbon chemical shift in the gramicidin channel, where it may be seen that two binding processes are being observed one at low (0.01–0.2 M) and the other at high (0.2–2 M) ion concentrations. The sigmoid curve for a single binding process is included to demonstrate how significantly the experimental data varies from a single binding process. The standard deviation for the chemical shift has been established at ± 0.06 ppm.³¹

TLC, amino acid analysis, high-pressure liquid chromatography, and ^{13}C nuclear magnetic resonance spectroscopy.⁴⁸

Sample Preparation and Handling. Preparation of gramicidin channels packaged into lyso-PC structures was by means of the sonication and heat incubation procedure previously described.^{32,42} In Figure 1 are given the circular dichroism spectra of the lyso-PC packaged ($1\text{-}^{13}\text{C}$) Trp^{13} gramicidin A (part A) and the natural gramicidin (part B) where it may be seen that both preparations have achieved the proper channel state necessary for ion interaction.^{42,49} Concentrations of the channel packaged into the lipid were determined by UV spectrophotometry after removing any unincorporated peptide by centrifugation and were found to be 2.87 and 3.16 mM for the samples used in the chemical shift and relaxation time experiments, respectively.

Before proceeding with the characterization of binding to the channel by rubidium-87 NMR, it is of interest to determine whether all of the gramicidin molecules are equally accessible to the ion in this particular system. It has been shown by selective carbonyl carbon ^{13}C enrichment that the location of the monovalent ion binding site in the channel is between the carbonyl carbons of Trp^{11} and $\text{Trp}^{13}\text{-GA}$.⁴¹ By observing one of these carbonyl carbon resonances in the presence of rubidium ion, it is possible to determine the nature of the interaction reported by a channel resonance. In Figure 2 is shown the carbon-13 spectra of ($1\text{-}^{13}\text{C}$) Trp^{13} gramicidin A with and without rubidium ion present. The broad resonance centered at 170.2 ppm with no ion present of the labeled carbonyl in the channel is observed to shift downfield by 1 ppm upon addition of 1 M RbCl . Although the signal is broad (in comparison with that of the lipid $\text{C}=\text{O}$ at 173.9 ppm), it may be seen that essentially the entire resonance shifts downfield upon ion interaction; therefore, it is reasonable to consider that all of the channels are accessed by the ion and the analytical concentration determined by UV may be used in the

binding constant analysis for the rubidium-87 data.

NMR experiments were performed on samples placed in calibrated 0.5-mL microcells inserted into 10-mm tubes (Wilmad Glass Company, Buena, NJ). Addition of rubidium ion to the samples was achieved by introduction of RbCl salt which had been stored in a vacuum oven and then by vortexing to ensure mixing. Samples containing gramicidin channels were incubated at 70 °C for 10 min to ensure equilibration of the ion with the lipid bilayer system. Data for the rubidium ion, free and in the presence of the lipid, were collected on samples diluted from a 1 M RbCl stock solution in $^2\text{H}_2\text{O}$ and on a concentration of lysolecithin equivalent to that of the gramicidin preparations.

Instrumentation. A JEOL FX-100 spectrometer equipped with a 10-mm multinuclear probe operating at 32.6 MHz with an internal deuterium lock was used to collect the rubidium-87 data. Temperatures in the probe were maintained at 30 ± 2 °C by a JEOL VT-3B temperature controller and were measured subsequent to each data acquisition by a home-built temperature probe inserted directly into the sampling area. As the line width of rubidium-87 in aqueous solution is very broad (>100 Hz in $^2\text{H}_2\text{O}$) and was observed to be many times broader in the presence of the channel, a spectral width of 25 KHz (sampling interval of 40 μs) was used to collect spectra. Due to the rapid transverse relaxation time of rubidium-87, it is necessary to begin data acquisition as soon as possible after the transmit pulse ends; however, some acoustical ringing in the probe was encountered which became transformed into a serious base line roll in the frequency spectrum. Instrumental conditions were therefore adjusted on a microcell containing a $^2\text{H}_2\text{O}$ blank until a straight base line was observed. A minimum delay time of 20 μs was required to achieve this condition.

The inversion recovery ($180^\circ\text{-}\tau\text{-}90^\circ$) pulse sequence was used to measure the rubidium-87 longitudinal relaxation times with a pulse repetition delay of at least $10T_1$ for complete relaxation and with use of eight to nine different pulse intervals, τ , in calculating the experimental values. Pulse widths for inversion of the magnetization were determined for each T_1 measurement and were typically 50 ± 2 μs . Partially relaxed spectra near the null point of the magnetization recovery were collected subsequent to each T_1 measurement and required approximately 10 to 30 times more accumulations than the inversion recovery spectra to achieve an adequate spectral signal-to-noise ratio.

Background Data on Rubidium-87. In order to characterize the interaction of rubidium ion with the gramicidin channel it is necessary to first determine the relevant NMR parameters for RbCl in $^2\text{H}_2\text{O}$ and in $L\text{-}\alpha\text{-lysolecithin}$ in $^2\text{H}_2\text{O}$. The concentration dependence of RbI in $^2\text{H}_2\text{O}$ has been reported by others;³⁵ however, for the work presented here chemical shift as well as relaxation time dependence on chloride salt concentration should be examined. The rubidium-87 chemical shift in $^2\text{H}_2\text{O}$ moves downfield, or to more positive values, on increasing RbCl concentration as seen in Figure 3A. Also, in the presence of lyso-PC there is a slight, constant shift in the same direction. The chemical shift in the presence of channels is reported after subtracting the contribution of the lipid at the same ion concentration—all samples being measured with 10 mM RbCl in $^2\text{H}_2\text{O}$ as the reference. Concentration dependence of the longitudinal relaxation time for $^{87}\text{RbCl}$ in $^2\text{H}_2\text{O}$ and in lyso-PC is given in Figure 3B. For aqueous rubidium ion the T_1 is approximately 2.25 ms with a slight increase in T_1 on increasing concentration. The longitudinal relaxation time in the presence of lipid, $T_1(\text{l})$, drops slightly from that of the free ion with the same general slope to the curve. A mean value of 2.0 ms for $T_1(\text{l})$ was used in analyzing the channel data. Also included in Figure 3B are a few T_1 values collected on the lysolecithin-gramicidin system (+) to illustrate the change in magnitude of the rubidium-87 relaxation time caused by interaction with the channel.

Data Analysis. Chemical Shift. From an analysis of the variation of the Rb chemical shift with RbCl concentration, the binding constant and the chemical shift at the binding site may be estimated by using a one-site model. Assuming fast exchange, the observed chemical shift may be written as

$$\delta = P_f\delta_f + P_b\delta_b \quad (1)$$

where δ_f and δ_b are the chemical shifts of the ion respectively at free and bound sites. P_f is the ion fraction at "free" site f while P_b is that at the bound site b . If the chemical shifts are measured with respect to the free site, then one might set $\delta_f = 0$. Equation 1 simplifies accordingly to

$$\delta = P_b\delta_b \quad (2)$$

If K_b is the binding constant of the ion for site b , then

$$P_b = [\text{Rb}]_b / [\text{Rb}]_T \quad (3)$$

where the concentration of the bound ion is given by

$$[\text{Rb}]_b = \frac{1}{2}([\text{G}]_T + [\text{Rb}]_T + K_b^{-1}) - \frac{1}{2}([\text{G}]_T + [\text{Rb}]_T + K_b^{-1})^2 - 4[\text{G}]_T[\text{Rb}]_T^{1/2} \quad (4)$$

(48) Urry, D. W.; Trapane, T. L.; Romanowski, S.; Bradley, R. J.; Prasad, K. *Int. J. Pept. Protein Res.* **1983**, *21*, 16–23.

(49) Masotti, L.; Spisni, A.; Urry, D. W. *Cell Biophys.* **1980**, *2*, 241–251.

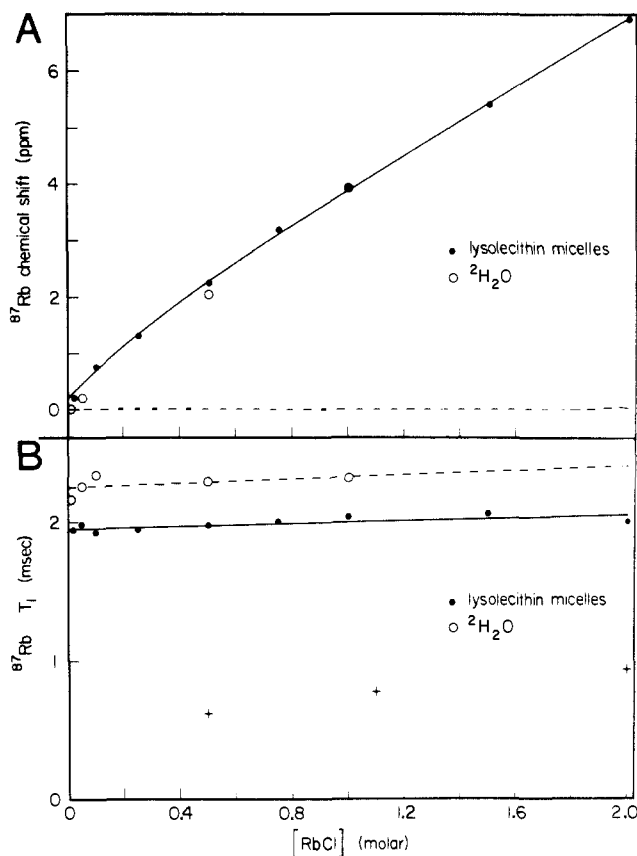


Figure 3. (A) ^{87}Rb chemical shift dependence at 30 °C on RbCl concentration for $^2\text{H}_2\text{O}$ (O) and for L- α -lysolecithin in the $^2\text{H}_2\text{O}$ (●). The signal from 10 mM RbCl in $^2\text{H}_2\text{O}$ was used as the reference. (B) ^{87}Rb longitudinal relaxation time (T_1) dependence at 30 °C on RbCl concentration for $^2\text{H}_2\text{O}$ (O) and for lysolecithin in $^2\text{H}_2\text{O}$ (●). The concentration of the lipid in parts A and B is the same as that used in the lyso-PC-GA samples. A few experimental values (+) obtained on the gramicidin system are included to illustrate the decrease in the T_1 of the rubidium ion on interaction with the channel.

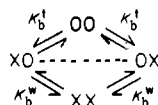
as a function of K_b , the total ion concentration $[\text{Rb}]_T$, and the total gramicidin monomer concentration $[\text{G}]_T$.

From observed Rb ion concentration dependence of the chemical shift, the one-site binding constant, K_b , and the chemical shift at the binding site, δ_b , may be estimated by non-linear least-squares fitting of the calculated chemical shift, δ_{calcd} , using 2–4 to the observed chemical shift, δ_{obsd} . The fitting is achieved in practice by minimizing the discrepancy R with respect to K_b and δ_b by using a quasi-Newton optimization routine. The summation in eq 5 is over various Rb ion concentrations with

$$R = \frac{1}{N} \left[\sum_{i=1}^N (\delta_{\text{calcd}} - \delta_{\text{obsd}})^2 \right]^{1/2} \quad (5)$$

N being the total number of data points collected in the titration.

It is necessary to note here that the binding constant, K_b , so obtained with use of a one-site model should be properly scaled since it is an interacting two-site model that is appropriate for the gramicidin channel. Each empty channel contains two identical "tight" binding sites and an ion occupying one site converts the other site into a "weak" site. The two-site model may be delineated by the scheme where OO, XO, OX, and



XX are the empty, singly and doubly occupied channel states.

If K_b^w is much smaller than K_b^t , then the binding process relevant at low ion concentrations is the tight binding process given by K_b^t which can be expressed as

$$K_b^t = \frac{[\text{XO}]}{[\text{Rb}][\text{OO}]} = \frac{[\text{OX}]}{[\text{Rb}][\text{OO}]} = \frac{[\text{XO}] + [\text{OX}]}{2[\text{Rb}][\text{OO}]} \quad (6)$$

But $([\text{XO}] + [\text{OX}])/([\text{Rb}][\text{OO}])$ is the binding constant for the lumped process

OO (empty channel) \rightleftharpoons OX (singly bound channel)

which must be equal to K_b obtained from the one-site analysis at low ion concentration where the double occupancy of the channel is negligible. Therefore

$$K_b^t = \frac{1}{2} K_b \quad (7)$$

Line Shape Analysis. According to the theoretical treatment of Bull²⁴ the signal from a spin- $3/2$ nucleus can consist of two Lorentzians of different line widths; due to quadrupolar relaxation the intensities of the broad and the narrow components are expected to be in the ratio of 60:40. Furthermore, their line widths are related to the correlation time, τ_c , at the binding site as given by the following equation:

$$\frac{1/T_2' - 1/T_{2f}}{1/T_2'' - 1/T_{2f}} \approx \frac{1 + (1 + \omega^2\tau_c^2)^{-1}}{(1 + 4\omega^2\tau_c^2)^{-1} + (1 + \omega^2\tau_c^2)^{-1}} \quad (8)$$

where T_2' and T_2'' are the transverse relaxation times of the broad and narrow components, respectively. When the signal is found to be made up of two Lorentzians, fitting the observed signal to the sum of two Lorentzians, gives T_2' and T_2'' . Then with use of eq 8, an estimate for the correlation time, τ_c , is obtained.

From an analysis of eq 8, it is apparent that the signal can be distinctly multiple-Lorentzian, whenever the correlation time, τ_c , is longer than a few ns. Since earlier studies at high sodium ion concentration show that the correlation time is in this range,^{28–30} the ^{87}Rb signal may also be expected to be made up of two Lorentzians at high ion concentration.

Calculation of Rubidium Activity Coefficients. The activity coefficients were obtained for RbCl at 25 °C for the concentration range of 0.5 mM to 2 M by fitting the experimental activity coefficients reported by Harned and Owen⁵⁰ to a four-parameter Guggenheim equation. The following equation was found to reproduce experimental values listed by Harned and Owen⁵⁰ quite well in the range of ion concentration employed in this study.

$$\log(\text{activity coefficient}) = \frac{-0.54\sqrt{m}}{1 + 1.32\sqrt{m}} - 0.002267m + 0.00231m^2 \quad (9)$$

where m is the molality.

Results

Longitudinal Relaxation Studies. A stack of partially relaxed Fourier transformed (PRFT) spectra using the inversion recovery method for rubidium-87 in the presence of 3.16 mM channels is given in Figure 4. This demonstrates the quality of the spectra and the spectral widths, and most significantly it demonstrates the presence of both narrow and broad components. Specifically at pulse interval of 0.595 ms, it is apparent that the narrow component has inverted and become positive while the broad component is yet negative. In a standard analysis of T_1 , the total peak height at the frequency of maximal intensity, M_z , is fitted to the expression

$$M_z(\tau) = M_0[1 - 2 \exp(-\tau/T_1)] \quad (10)$$

for each value of pulse interval, τ , to obtain T_1 where M_0 is the line intensity at infinite τ . In Figure 5 these values of T_1 are then used to plot the inverse excess longitudinal relaxation rates over that obtained in the presence of lyso-PC alone (Figure 3) in a James-Noggle plot.²⁶ The accessible ion activity range was 0.5 to 1.5 M RbCl, and the inverse of the negative x -axis intercept provides an apparent binding constant. This provides an estimate of the weak binding constant, K_b^w , of 1 M^{-1} . Interestingly, the carbon-13 NMR chemical shift titration carried out at 70 °C, given as the insert in Figure 2, shows a second sigmoidal change in chemical shift which is centered at about 1 M; this again defines a binding constant of approximately 1 M^{-1} .

For sodium ion, however, increasing temperature from 30 to 75 °C resulted in a decrease in binding constant by a factor of 2 or 3.⁵¹ Also it is necessary to determine whether the overlapping of both narrow and broad components might introduce some error in the estimation of binding constants. The pulse interval for

(50) Harned, H. S.; Owen, B. B. *The Physical Chemistry of Electrolyte Solutions*, 3rd ed.; Reinhold Publishing Corp.: New York, 1967.

(51) Urry, D. W.; Trapane, T. L.; Venkatachalam, C. M.; Prasad, K. U. *Int. J. Quantum Chem.: Quantum Biology Symp.* 1986, 12, 1–13.

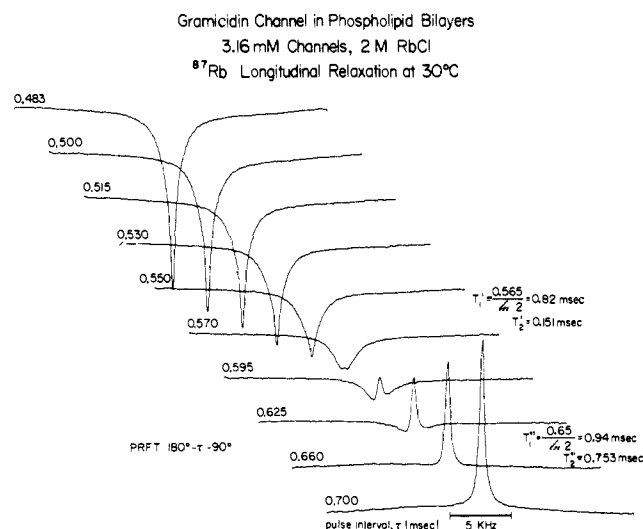


Figure 4. Partially relaxed inversion recovery ($180^\circ-\tau-90^\circ$) spectra measured with pulse intervals, τ , passing through the inversion, or null, point of the longitudinal magnetization for an activity of 1.54 M RbCl (i.e., a concentration of 2.0 M) in the presence of 3.16 mM gramicidin channels. Two distinct line shapes are observed, each passing from negative to positive magnetizations at different times. The narrow signal inverts first at approximately 0.565 ms followed by the broad component inversion at 0.65 ms. These null intervals correspond to relaxation times for the two components of $T_1' \approx 0.82$ ms and $T_1'' \approx 0.94$ ms, and from the line widths at half intensity at the null times for the opposite component $T_2' = 0.151$ ms and $T_2'' = 0.753$ ms.

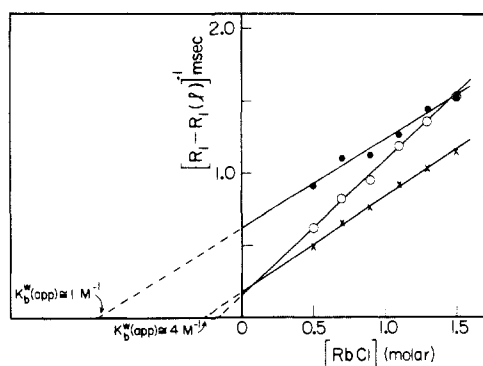


Figure 5. James-Noggle plot of the excess longitudinal relaxation rates for rubidium-87 ion interaction with 3 mM lysolecithin packaged gramicidin A channels. Relaxation times were experimentally measured in three ways: from the standard inversion recovery method (\bullet) and from the null times of the broad (\circ) and narrow (\times) signal components (see Figure 4). Linear analysis of the three curves gives an apparent binding constant (for the rubidium ion at high concentrations) of $K_b^w \approx 1$ to 4 M^{-1} .

inversion of each component can be reasonably estimated directly from the spectra such that T_1' and T_1'' can be obtained separately. As indicated in Figure 4, the null point of the narrow component at an ion activity of 1.54 M RbCl is very near the pulse interval of 0.570 ms and is estimated to be at 0.565 ms by interpolation which gives a T_1' of 0.82 ms. The null point of the broad component is observed near the pulse intervals of 0.660 ms and is estimated to be 0.65 ms to give a T_1'' of 0.94 ms. These values were determined at each ion concentration and each were plotted as inverse excess relaxation rates in Figure 5. The two separate plots, within the accuracy of their determination, gave similar negative x -axis intercepts and indicate that the weak binding process could be approximated by $K_b^w \approx 4$ M^{-1} . This reasonably places a weak binding constant in the range of 1 to 4 M^{-1} .

Chemical Shift Data. As seen in Figure 6, rubidium-87 gives a large negative chemical shift on interaction with the gramicidin channel. It is appreciated from the previous ion and carbon-13 NMR studies (see Discussion) that there are two discernible binding constants and binding sites. Accordingly a fit of Figure

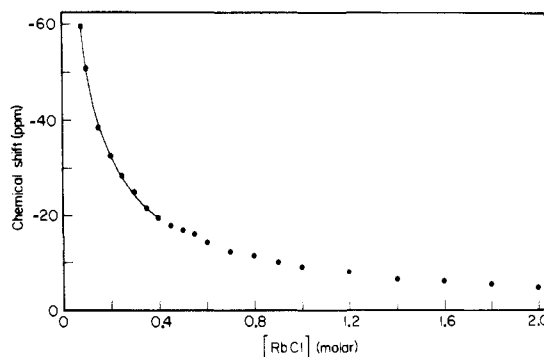


Figure 6. Concentration dependence of ^{87}Rb chemical shift at 30°C in the presence of 2.87 mM lysolecithin packaged gramicidin channels. The reference is 10 mM RbCl in $^2\text{H}_2\text{O}$ and the chemical shift contribution of the lyso-PC has been subtracted at equivalent ion concentrations (see Figure 3 and Methods). The experimental data at low values, 80–400 mM RbCl, has been analyzed according to a single binding process. The best fit to the data gives a K_b of 16 M^{-1} and is represented by the solid curve.

6 would require four parameters, the two binding constants and a binding site chemical shift for single ion occupancy and a second chemical shift value for double ion occupancy. The problem of estimating the weak binding constant becomes particularly difficult at high ion concentrations where the ratio of bound to free ions is so very small. Recognizing a weak binding constant in the 1 to 4 M^{-1} range, the chemical shift data were fitted only in the concentration range of 80 to 400 mM (see the calculated solid line) to give an apparent tight binding constant of 16 M^{-1} and a chemical shift for single ion occupancy of -1000 ppm. As there is limited low concentration data (when compared to sodium-23 chemical shift data which starts, for example, at 0.5 mM) and as there could be some influence of the weak site, this is expected to be a minimal value for the magnitude of the tight binding constant. In fact a fit to the carbon-13 chemical shift data in Figure 2 gave a value of 28 M^{-1} at 70°C (unpublished) and again, as with sodium binding,⁵¹ a value of about twice that magnitude would be expected at 30°C . Accordingly it is reasonable to consider a tight binding constant of greater than 30 M^{-1} for 30°C .

Line Shape Analysis. It was demonstrated in Figure 4 that there are two components in the rubidium-87 resonance line. This is the case only in the presence of channels and not in the presence of the phospholipid alone. It also appears that the line shape is Lorentzian at low ion concentration in the presence of channels. While this latter conclusion is made difficult by the 5-kHz line width at 100 mM RbCl, the ratio of line width at half-intensity to that at one-eighth intensity, $\nu_{1/8}/\nu_{1/2}$, is clearly less than 3, and for a true Lorentzian line it should be $\sqrt{7}$, i.e., 2.65.⁵² In the case of sodium-23 there is only a simple Lorentzian line shape below 100 mM NaCl in the presence of channels, yet there is a tight binding constant due to an ion entering the channel.^{29,30,41} One way for this to occur would be for $\omega\tau_c$ to be less than one, implying a rapid exchange with the channel (see below). With the evidence for a relatively low central barrier (i.e., a rapid intrachannel ion translocation from one binding site at one end of the channel to the second ion binding site at the other end of the channel), such a rapid exchange should result in high currents of greater than 10^7 ions/s at 100 mM NaCl.²⁸ This is not the case for gramicidin A which requires the view that the first ion enters the channel but leaves relatively much more slowly than at higher concentrations. An estimate of the off-rate constant for single ion occupancy of 3×10^5 s^{-1} has been obtained for sodium ion from a plot of line width vs. ion chemical shift.²⁸⁻³⁰ This interpretation for sodium ion is supported by integration data indicating loss of about half of the resonance area at 50 mM NaCl in the presence of channels as compared to 50 mM NaCl in water (R. B. McMichens and D. W. Urry, unpublished data).

(52) Laszlo, P. *Angew. Chem., Int. Ed. Engl.* **1978**, *17*, 254–266.

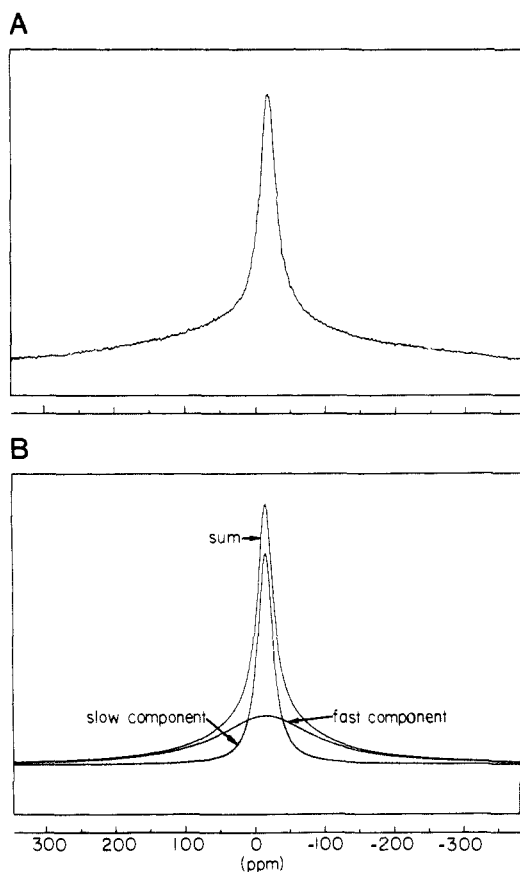


Figure 7. (A) Rubidium-87 nuclear magnetic resonance spectrum at 32.6 MHz and 30 °C for the lysolecithin packaged natural gramicidin A. The concentrations of channel and RbCl are 2.87 and 550 mM, respectively, and the chemical shift is given in reference to 10 mM RbCl in $^2\text{H}_2\text{O}$. Note the obvious complex Lorentzian shape of the resonance signal. (B) Calculated curve obtained after deconvolution of the above spectrum into two Lorentzian line shapes. The line width at half-intensity for the broad, or fast, component (60% of total area) is 5500 Hz and that for the narrow, or slow, component (40% of total area) is 850 Hz. Also shown is the sum of both calculated curves which compares very well with the experimentally observed line shape. With $T_2 = (\pi\nu_{1/2})^{-1}$, this gives $T_2' \approx 0.058$ ms and $T_2'' \approx 0.37$ ms. By comparison with Figure 4, it may be noted that the broad (faster) component in T_2 is the slower component with respect to T_1 .

In the present case of rubidium ion the resonance areas of 100 mM RbCl in D_2O and in the lysolecithin–gramicidin system were also compared by means of integration. Each sample was accumulated for the same number of scans. Then the integrals were compared by setting 100 mM RbCl in D_2O as the standard integral value and comparing it to the sample with gramicidin present. Correction for the difference in normalized gain was achieved by dividing the integral obtained for 100 mM RbCl in the lysolecithin–gramicidin system by the normalized gain factor. The resonance area of 100 mM RbCl in the lysolecithin–gramicidin system was found to be 46% of the area of the 100 mM RbCl in D_2O . For the rubidium ion, therefore, it is not unreasonable to consider the double Lorentzian resonance line as arising under conditions of double occupancy and to be the result of a more rapid rubidium ion exchange with the channel under conditions of double ion occupancy.

From the fitting of the line shape at 550 mM RbCl (see Figure 7), the values for T_2' and T_2'' were determined to be 0.058 and 0.37 ms, respectively. When these values are used in the Bull expression (see eq 8 above) with $T_{2f} \approx T_{2(i)} = 1.9$ ms, the correlation time, τ_c , is calculated to be 1.3×10^{-8} s. The curve resolution of Figure 7 utilized a broad Lorentzian which extended beyond the 25 kHz observation window. This resolution can be checked at higher ion concentrations where the lines become less broad and where it is possible as in Figure 4 to find those values of pulse interval, τ , first for which the narrow component is nulled

and second for which the broad component is nulled. This is shown in Figure 4 for an ion activity of 1.54 M. From the line widths at half-intensity at a τ of $0.570 T_2' = 0.151$ ms and at a τ of $0.660 T_2'' = 0.753$ ms. It is useful to appreciate that the delay time used of 26 μs in this data collection is not such a significant part of the relaxation time for the broad component and that the base line is seen to be quite satisfactory. As with the curve resolution when these values are used in eq 8, the same $\tau_c = 1.3 \times 10^{-8}$ s is obtained.

The correlation time has been considered to arise from three processes:^{53–55}

$$\frac{1}{\tau_c} = \frac{1}{\tau_r} + \frac{1}{\tau_{\text{int}}} + \frac{1}{\tau_b} \quad (11)$$

where τ_r is the orientation correlation time for the ion binding site in the magnetic field, τ_{int} is the correlation time of the vibrating electric field gradient at the cation binding site, and τ_b is the ion occupancy time in the channel which is the inverse of the off-rate constant, k_{off}^w . As the ion binding site is in a large membranous system, τ_r would be long and would not contribute significantly to a correlation time of 13 ns.

In order to achieve further interpretation of τ_c , it is helpful to consider the temperature dependence of τ_c as previously obtained for sodium-23.⁵¹ When $-\log \tau_c$ is plotted vs. inverse temperature (K), following the Eyring rate theory formalism, it is found to be well-behaved presenting a linear plot with a ΔH^\ddagger of 5.9 kcal/mol and a ΔS^\ddagger of -5.4 cal/(mol-deg). Assuming this to be a vibrational process as would be required if τ_{int} were the dominant component of τ_c , it is possible to use the harmonic oscillator partition function to determine the vibrational frequency that would be relevant to an entropy of 5.4 cal/(mol-deg),⁵⁶ i.e.,

$$S_i = R \ln (1 - e^{-h\nu_i/kT})^{-1} + \frac{Nh\nu_i}{T} (e^{h\nu_i/kT} - 1)^{-1} \quad (12)$$

The vibrational frequency would be about 10^{12} s^{-1} . Such a vibrational process would have a correlation time of tenths of a picosecond rather than of nanoseconds observed for τ_c and would involve internal energies an order of magnitude lower than observed for τ_c . The temperature study with the resulting entropies and enthalpies of activation are not consistent with the characterization of a vibrational process and τ_{int} would therefore in this case appear not responsible for the several ns correlation time. This is perhaps due to the low symmetry of the binding site. On the other hand with $\tau_c^{-1} \approx \tau_b^{-1} = k_{\text{off}}^w$, these numbers are entirely appropriate for an off-rate constant. Importantly for the system under study the magnitude of $\tau_c^{-1} \approx k_{\text{off}}^w$ is just the magnitude required to describe the current passing through the channel as will be seen below.

Discussion

Comparison of Rubidium-87 NMR Data with That of Other Alkali Metal Ions. Quadrupolar ion NMR studies on each of the alkali metal ions are an effective means of developing information on binding constants and rate constants for interaction with the gramicidin channel. The relative strengths and weaknesses in studying the different group IA (group 1) ions in this regard are seen by comparing the changes in relaxation times and chemical shifts exhibited by these ions on interaction with the channel. The ratio of experimental T_1 in the presence of lyso-PC in $^2\text{H}_2\text{O}$ to that in the presence of 3 mM channels incorporated into lyso-PC in $^2\text{H}_2\text{O}$, i.e., $T_1(\text{lyso-PC})/T_1(\text{channels} + \text{lyso-PC})$ at 1 M ion

(53) Marshall, A. G. *J. Chem. Phys.* **1970**, *52*, 2527–2534.

(54) Bull, T.; Norne, J. E.; Reimarrsson, P.; Lindman, B. *J. Am. Chem. Soc.* **1978**, *100*, 4643–4647.

(55) Forsén, S.; Lindman, B. *Chem. Br.* **1978**, *14*, 29–35.

(56) Hagler, A. T.; Stern, P. S.; Sharon, R.; Becker, J. M.; Naider, F. *J. Am. Chem. Soc.* **1979**, *101*, 6842–6852.

(57) In this paper the periodic group notation in parentheses is in accord with recent actions by IUPAC and ACS nomenclature committees. A and B notation is eliminated because of wide confusion. Groups IA and IIA become groups 1 and 2. The d-transition elements comprise groups 3 through 12, and the p-block elements comprise groups 13 through 18. (Note that the former Roman number designation is preserved in the last digit of the new numbering: e.g., III \rightarrow 3 and 13.)

chloride, is 20 s/14 s = 1.43 for lithium-7, 48 ms/21 ms = 2.29 for sodium-23, 49 ms/4 ms = 12.3 for potassium-39, 2.0 ms/0.75 ms = 2.67 for rubidium-87, and 10.4 s/2.3 s = 4.52 for cesium-133. This means that the observed change required to estimate binding constants is as favorable or slightly more favorable for rubidium-87 than for sodium-23. The difficulty with rubidium-87 is the very short relaxation time which gives rise to very broad resonance lines which in turn result in sensitivity limitations when high-resolution spectrometers are used. This results in data not being obtainable at low ion concentrations where tighter ion binding processes would be observed. The magnitude of chemical shift exhibited by rubidium-87 on interaction with the channel is actually quite favorable. With use of lyso-PC in $^2\text{H}_2\text{O}$ as the reference, the chemical shift in the presence of 3 mM channels for 100 mM ion chloride is 0 ppm for lithium-7, -2.6 ppm for sodium-23, >|-30| ppm for potassium-39, -39 ppm for rubidium-87, and +0.06 ppm for cesium-133. While data at lower ion concentration are difficult to obtain for ^{39}K and ^{87}Rb , at 10 mM ion chloride the values are -9 ppm for ^{23}Na and +0.6 ppm for ^{133}Cs ; both of these chemical shifts are useful to estimate tight binding constants from low ion concentration data. It may be noted that only the cesium-133 ion gives a downfield chemical shift on entering the channel; this is thought to be due to ion pairing with chloride.³² The large negative chemical shift exhibited by rubidium suggests that ion pairing with chloride is not a significant factor for rubidium. Thus in spite of limitations in obtaining data at low ion concentrations, useful chemical shifts are observed. It should not be assumed when there is multiple ion binding, however, that fitting of data in any particular accessible range gives a true value for a binding constant.

Binding Constant Information. The early sodium-23 NMR studies²⁸⁻³⁰ on the lyso-PC-channel system provided evidence for two binding constants (a tight binding constant, K_b^w , and a weak binding constant, K_b^o); this was apparent in analysis of the T_1 data, of line width data, and of the low concentration range of the chemical shift data. Consistent with this, T_1 analyses of cesium-133 binding also showed two binding constants.³² That both binding processes were indeed due to ion interactions with the channel was confirmed by following the ion induced carbonyl carbon chemical shift of synthetic gramicidin A molecules in which either the Trp¹¹ or the Trp¹³ carbonyl carbon was 90% enriched. This has been demonstrated for thallium ion and for potassium ion at 70 °C.³¹ As shown in the insert for Figure 2, the rubidium ion induced carbonyl carbon chemical shift also exhibits two binding processes. Accordingly it can be argued that there are two binding constants for rubidium ion interaction with the channel in spite of the fact that the present instrumentation cannot observe lower concentrations than 500 mM [RbCl] for the T_1 studies and 100 mM [RbCl] for the chemical shift studies.

As noted in the Results section, a James-Noggle plot²⁶ in the 500 mM to 1.5 M activity range results in estimates for the weak binding process of between 1 and 4 M^{-1} , and fitting the ^{87}Rb chemical shift data in the 100 to 400 mM range gives an apparent binding constant of 16 M^{-1} . Since it was not possible to go to lower ion concentration where the tight site would be more pronounced and the ratio of bound to free ions more favorable, it can be expected that this tight binding constant is a minimal value. Indeed fitting of the carbon-13 chemical shift data of Figure 2 (unpublished results) indicates a value of 30 M^{-1} or more for K_b^t . The ^{87}Rb NMR derived values of greater than 16 M^{-1} for K_b^t and in the range of 1 to 4 M^{-1} for K_b^o are to be compared to the values estimated by Eisenman et al.⁹ of 57 and 0.9 M^{-1} from fitting of conductance data. Accordingly, the ^{87}Rb NMR derived values are quite reasonable.

Rate Constant Information and Single Channel Currents. From the data of Figures 4 and 7 and the Bull analysis,²⁴ the ion correlation time was estimated to be 1.3×10^{-8} s, and with the obviously long reorientation correlation times for the membranes in which the channel is incorporated and with the evidence presented in the Results section that τ_c is not due to a vibrational process, this translates into an off-rate constant, k_{off}^w , of 7.7×10^7 s^{-1} . From the data in Figure 5, the binding constant for achieving double occupancy, i.e., for the weak site, K_b^w , is in the range of 1 to 4 M^{-1} . Since $K_b^w = k_{\text{on}}^w/k_{\text{off}}^w$, then $k_{\text{on}}^w = K_b^w k_{\text{off}}^w$. With this rate constant information, using the analysis previously discussed in detail for the sodium ion,²⁸⁻³⁰ recognizing at high RbCl concentration, e.g., 1 M, that concern need only be with the probability of the singly occupied channel, χ_s , and the probability of the doubly occupied state, χ_d , with $\chi_s + \chi_d = 1$; and realizing with a significant applied potential, e.g., 100 mV, that the initial entry barrier is rate limiting, then the single channel current, I , may be written at steady state by using the single barrier, i.e.,

$$I = \text{forward rate} - \text{backward rate} \quad (13)$$

$$I = [\text{Rb}^+] k_{\text{on}}^w \chi_s e^{l/zFE/2dRT} - k_{\text{off}}^w \chi_d e^{-l/zFE/2dRT} \quad (14)$$

$$I = \frac{K_b^w k_{\text{off}}^w}{1 + K_b^w} (e^{l/zFE/2dRT} - e^{-l/zFE/2dRT}) \quad (15)$$

The exponential term is the Eyring factor that introduces the voltage dependence where l is the distance from the minimum to the barrier ($l_f = l_b = 3$ Å); z is the charge on the ion; F is the Faraday, 23 kcal/(mol·V); E is the potential, 0.1 V; $2d$ is the total length of the channel, 30 Å; R is the gas constant, 1.987 cal/(mol·deg); and T is the absolute temperature, 303 K. Also with $\chi_s = (1 + K_b^w)^{-1}$, $\chi_d = K_b^w/(1 + K_b^w)$, and taking $[\text{Rb}^+] = 1$ M and $K_b^w = 1$ M^{-1} , the calculation of the single channel current, using NMR derived rate constants, becomes

$$I = \frac{1}{2} \times 7.7 \times 10^7 (e^{0.38} - e^{-0.38}) \text{ions/s} = 3 \times 10^7 \text{ions/s} \quad (16)$$

This converts, with 1.6×10^{-19} coulomb/ion, to a single channel current of 4.9 pA (picoamps) and, with an applied potential of 0.1 V, to a conductance, γ , of 49 pS (picosiemens). If the higher value for the weak binding constant of 4 M^{-1} were used, the conductance value would be 78 pS. The actual single channel conductance at 100 mV and 30 °C for 1 M RbCl is essentially the same as that for 1 M CsCl, i.e., 48 pS.³² That the calculated conductance using NMR derived rate constants is remarkably close to the experimental measurement of the single channel conductance gives credence to the NMR approach.

There is yet another comparison that may be made which again checks the utility of line shape analysis for deriving off-rate constants. This is a comparison of the off-rate constant for rubidium-87 with that obtained for sodium-23 at high ion concentration on the same system. The value of the former is, of course, 7.7×10^7 s^{-1} and that for the latter was previously reported to be 2.3×10^7 s^{-1} .³⁰ With both sodium ion²⁸⁻³⁰ and rubidium ion, weak binding constants close to 1 M^{-1} , a ratio of these rate constants, $k_{\text{off}}^w(\text{Rb}^+)/k_{\text{off}}^w(\text{Na}^+)$, would be expected to compare favorably with the conductance ratio, $\gamma(\text{Rb}^+)/\gamma(\text{Na}^+)$. The former is 3.35 whereas the latter is very close to 3.^{6,7} Again the NMR derived quantities compare well with the electrical measurements.

Acknowledgment. This work was supported in part by the National Institutes of Health (Grant GM-26898). We gratefully acknowledge the assistance of Ruth Brown McMichens on the NMR studies.